JABFM
eISSN 2280-8000

J Appl Biomater Funct Mater 2016; 14(2): e189-e196
DOI: 10.5301/jabfm.5000282

ORIGINAL ARTICLE

Open Access

Effect of the mineralizer solution in the hydrothermal synthesis of gadolinium-doped (10% mol Gd) ceria nanopowders

Gianfranco Dell'Agli[1], Luca Spiridigliozzi[1], Antonello Marocco[1], Grazia Accardo[2], Claudio Ferone[2], Raffaele Cioffi[2]

[1] Department of Civil and Mechanical Engineering and INSTM Research Unit, University of Cassino and Southern Lazio, Cassino, Frosinone - Italy
[2] Department of Engineering and INSTM Research Unit, University Parthenope of Naples, Naples - Italy

ABSTRACT

Background: Gadolinium-doped ceria is an attractive electrolyte material for potential application in solid oxide fuel cells (SOFCs) operating at intermediate temperatures typically with 10%-20% substitution of Ce^{+4} by Gd^{+3}. In particular, 10% gadolinium-doped ceria seems to have the highest values of conductivities among the other dopant compositions.

Methods: Nanosized powders of gadolinium-doped ceria were prepared by hydrothermal treatment using coprecipitate as a precursor and in the presence of 3 different mineralizer solutions. The powders obtained were characterized by X-ray diffraction analysis, scanning electron microscopy, transmission electron microscopy and thermal analysis, while the electrical behavior of the corresponding pellets were ascertained by AC impedance spectroscopy.

Results: Nanocrystalline gadolinium-doped ceria powders with fluorite cubic crystal structure were obtained by hydrothermal treatment. Independent of the mineralizer used, these powders were able to produce very dense ceramics, especially when selecting an optimized sintering cycle. In contrast, the electrical behavior of the samples was influenced by the mineralizer solution, and the samples synthesized in the neutral and alkaline solutions showed higher values of electrical conductivity, in the range of temperatures of interest.

Conclusions: By the coprecipitation method, it has been possible to synthesize nanosized gadolinium-doped cerium oxide in a fluorite structure, stable in a wide range of temperatures. Hydrothermal treatment directly on the as-synthesized coprecipitates, without any drying step, had a very positive effect on the powders, which can be sintered with a high degree of densification, especially with an optimized sintering cycle. Furthermore, the electrical behavior of these samples was very interesting, especially for the samples synthesized using neutral mineralizer solution and basic mineralizer solution.

Keywords: Fuel cells, Gadolinium-doped ceria, Hydrothermal treatment, Sintering

Introduction

Conventional solid oxide fuel cells (SOFCs) must operate above 800°C when electrolyte based on yttria-stabilized zirconia is used. Because of this, it is necessary to use costly materials for other components of the SOFC. Thus, lowering the temperature of SOFCs has been one of the main targets for recent research (1). From this point of view, ceria-based ceramics represent promising materials (2). Highly abundant, cerium oxide (CeO_2) is an important inorganic material because it can be used in various applications as a 3-way catalytic support for the elimination of toxic auto exhaust gases, for low-temperature water–gas shift (WGS) reactions, and as an oxygen sensor, fuel cell electrolyte, glass-polishing material etc. (3).

The oxygen vacancy concentration of ceria and relative oxide ion conductivity can be increased by the substitution of a lower-valence metal ion (i.e., R^{3+} ions with R = Gd, Sm, Nd, Y, Pr etc.) for cerium ions. For the enhancement of ionic conductivity of ceria, dopants which have ionic radii very close to cerium are normally selected.

Among the various ceria-based ceramics, gadolinium-doped ceria in particular is an attractive electrolyte material for potential application in SOFCs operating at intermediate temperatures, typically with the substitution of Ce^{+4} by

Accepted: February 2, 2016
Published online: May 6, 2016

Corresponding author:
Gianfranco Dell'Agli
Department of Civil and Mechanical Engineering
University of Cassino and Southern Lazio
Via G. Di Biasio 43
03043 Cassino (FR), Italy
dellagli@unicas.it

Gd^{+3} in the range 10%-20% at. In fact the very similar value of ionic radius between the host (Ce^{+4} ion) and the dopant (Gd^{+3} ion) in the cubic fluorite-type lattice gives rise to high ionic conductivity and low activation energy due to small binding energies for associates between oxygen vacancies and Gd^{+3} (4).

However, one of the main drawbacks of ceria-based materials is related to the high temperature required to obtain sintered materials of high density (2). Therefore, for these applications, it is important to obtain ultrafine powders. Several chemical routes have been proposed in the literature; in fact, it is well known that chemical techniques have the following advantages over the conventional ceramic processing techniques: high purity, high homogeneity and ultrafine powder (5-9).

Among the chemical routes, the hydrothermal process has attracted a lot of attention for the direct synthesis of crystalline ceramic powders at relatively low temperatures (10). In fact, hydrothermal treatment is one of the most efficient methods of soft chemistry in producing advanced materials with a controlled size and shape. Hydrothermal synthesis is ideal to prepare very fine powders characterized by high purity, controlled stoichiometry, high quality, narrow particle size distribution, controlled morphology, uniformity, low defect concentrations, high crystallinity, excellent reproducibility, high reactivity/sinterability and so on (11). In this context, the authors have extensively applied hydrothermal synthesis at low temperatures, mainly in the range 110°C-140°C, to produce nanosized ceramic powders, both in zirconia-based ceramics and in titania-based ceramics. In particular, both fully or partially stabilized zirconia doped with various cations – i.e., Y^{+3}, Yb^{+3}, Sc^{+3} or Ca^{+2} – and of various compositions for functional and structural applications (12-19), as well as ZrO_2-doped titania (20) have been synthesized with the low-temperature hydrothermal treatment.

From this point of view, the hydrothermal synthesis of ceria-based ceramics has been a promising research field in recent years (10, 21-26). Several different methods of carrying out the hydrothermal treatment have been proposed: without precipitating agent, i.e., directly on the solution of soluble cerium salt, onto xerogel or onto gel without washing/drying steps, at various temperatures and in the presence of different mineralizer agents. In all of these works, it can be deduced that nanosized particles of ceria or doped ceria are obtained by hydrothermal synthesis. However, the high temperature of the synthesis is a major drawback (26).

Therefore, the aim of the present work was the synthesis by hydrothermal treatment at low temperature (i.e., 140°C) of ceramic powders formed by gadolinium-doped ceria with 10% mol Gd^{+3} (CGO, in the following), using a hydrous cerium-gadolinium oxide coprecipitate as a precursor and in the presence of 3 different mineralizer solutions: acidic solution (with HCl) at pH 1, deionized water and basic solution (with KOH) at pH 13. The effect of the mineralizer solution on the hydrothermal synthesis of CGO and on its electrical behavior was evaluated. The sintering behavior of the hydrothermally synthesized powders was compared with that of the hydrous cerium-gadolinium oxide coprecipitate, to evaluate if there was a positive effect of the hydrothermal treatment on the sinterability of the nanosized powders. Furthermore, an optimized sintering cycle is proposed.

Methods

Cerium(III) nitrate ($Ce(NO_3)_3 \cdot 6H_2O$ 99.0%; Carlo Erba, Italy) and gadolinium nitrate ($Gd(NO_3)_3 \cdot 6H_2O$ 99.0%; Carlo Erba, Italy) were used as starting materials for the synthesis of hydrous cerium-gadolinium oxide by coprecipitation, with the following composition in the anhydrous form: $Ce_{0.9}Gd_{0.1}O_{1.95}$. The proper amounts of cerium and gadolinium salts were dissolved in deionized water make the total cationic concentration equal to 0.1 M, and then the solution was vigorously stirred for 1 hour. The coprecipitation was carried out by reverse precipitation – i.e., the solution containing dissolved cerium and gadolinium salts was slowly added to an excess ammonia solution (~4 M) under vigorous stirring. The coprecipitate was filtered and washed repeatedly with deionized water to remove the undesired ions. A part of this batch was dried overnight at 60°C, and this xerogel is referred to as sample C in the following. The gadolinium-cerium oxide content in sample C was determined by thermogravimetric analysis (TGA). Another part of the batch was directly used as a precursor in the various hydrothermal syntheses.

Conventional hydrothermal synthesis was carried out at 140°C for 1 day; the ratio between precursor and mineralizer was selected in such a way that there was 1 g of anhydrous CGO over 50 mL of mineralizer solution. The correct amount of hydrous gel and mineralizer was transferred to a sealed Teflon vessel (100 mL) held in an outer pressure vessel made of stainless steel. The vessels were rotated in an air thermostated oven at 25 rpm to mix the gel precursor with mineralizer solution during the treatment. After the hydrothermal treatment, the products were filtered, washed repeatedly with deionized water and finally dried overnight at 60°C. Three different mineralizer solutions were used, for 3 different treatment environments – acidic, neutral and basic. For the first one, a solution of 0.1 M of hydrochloric acid (sample H_A in the following) was used, for the second, pure deionized water (sample H_N in the following) and for the last one, a solution of 0.1 M of potassium hydroxide (sample H_B in the following).

The powders were compacted into cylindrical pellets by cold isostatic pressing (ABB, CIP 32330-P2 model) at 160 MPa. The sintering of these compacts was carried out in air at 1500°C for 3 hours.

The apparent density of the sintered compacts was calculated by mass measurements and geometrical considerations. This procedure did not introduce any great error into the density evaluation, because of the regular cylindrical shape of the specimens.

All of the samples were characterized by X-ray powder diffraction (XRD) using a Panalytical X'PERT MPD diffractometer to detect the crystalline phases of the products. The XRD analysis at high temperature (up to 1200°C) was carried out by an Anton Paar HTK 16 in air. Primary particle size of cubic CGO was calculated by the following formula (Scherrer formula):

$$d = K\lambda/(B\cos\theta)$$

where K is the shape factor, which varies with crystal shape (for spherical particles, its value is 0.89); λ is the wavelength

of the X-ray used (0.1541 nm for X-ray wavelength of CuKα); θ is the Bragg's angle of the (111) peak of cubic ceria; and B is the full width at half maximum (FWHM) of the (111) peak corrected for the instrumental broadening. To carry out this correction, B is calculated as $B_{sample} - B_{instr}$, where B_{instr} is determined using standard polycrystalline silicon. Both the fit profile, made using the pseudo-Voigt function, and the calculations related to the Scherrer formula were carried out using the software X'Pert HighScore of Panalytical.

The thermal behavior of the samples was ascertained by simultaneous differential scanning calorimetry and thermogravimetric analysis (DSC and TGA; Thermoanalyzer STA 409; Netzsch) in air at a heating rate of 10°C/min up to 1200°C and using αAl_2O_3 as a reference.

The specific surface area of products was determined by the BET method using a Micromeritics Gemini apparatus and utilizing nitrogen as an adsorbate, after drying the powders under vacuum at 100°C.

The morphology of the synthesized powders was observed by scanning electron microscopy (SEM; FEI Quanta 200; FEG) and by transmission electron microscopy (TEM; FEI Tecnai G2; Spirit Twin). The microstructure of the sintered pellets was observed by SEM, while the energy-dispersive X-ray (EDX) analysis was performed using an Energy Dispersion Spectrometer Oxford Inca Energy System 250 equipped with an INCAx-act LN2-free detector, working at 20 kV. To reveal the microstructure of the sintered pellets by SEM, one side of each was initially ground using a 30-µm diamond wheel and then polished to a 1-µm diamond finish. Furthermore, after polishing, the sintered pellets were also thermally etched at 1350°C for 1 hour.

Electrochemical impedance spectroscopy measurements were performed on a symmetric cell configuration. The electrodes were realized by painting the dense pellet surfaces with an Au paste. The Au-layered pellet was sintered at 600°C for 1 hour. The samples then sandwiched between 2 gold foils from which the contacts were taken out for the measurements. Characterization was performed in the range 500°C-800°C using a Solartron 1260 frequency response analyzer (FRA), coupled with a Solartron 1296 dielectric interface. The frequency was varied between 0.2 and 2 MHz, with a 100-mV alternate signal for all sintered pellets.

Results and discussion

Gadolinium-doped ceria coprecipitate

From the X-ray diffraction pattern of the sample C (not reported here) it was evident that sample C was partially amorphous and partially crystallized in the fluorite cubic crystal structure (ICDD card no. 01-075-0161 used for reference, related to $Gd_{0.1}Ce_{0.9}O_{1.95}$ with space group Fm-3m). The diffraction peaks of the cubic ceria were clearly visible albeit very broad. The dissolution of Gd into CeO_2 was ascertained by EDX analysis, and the measured Ce/Gd ratio was higher than 8, very close to the nominal value of 9. Further details are reported in the section "Sintering Cycles." The behavior of the precipitating gadolinium-doped ceria hydrous gel was different from that of other amorphous precipitate – i.e., zirconia hydrous gel (19) –and a significant amount

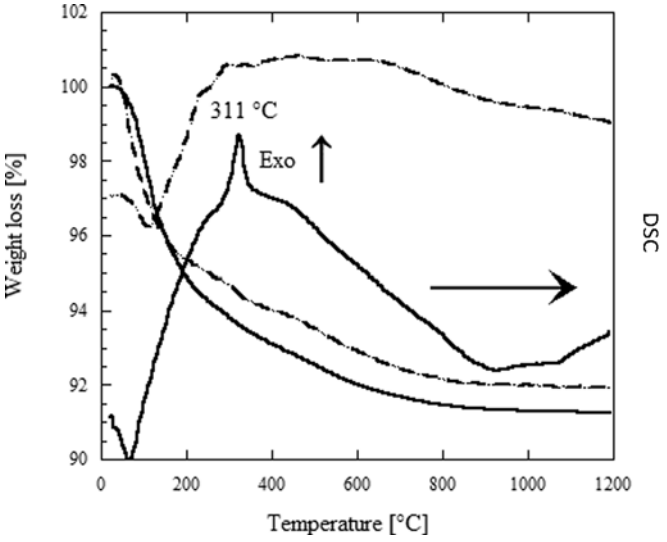

Fig. 1 - Differential scanning calorimetry and thermogravimetric analysis (DSC-TGA) thermograph of sample C (solid line) and sample H_N (dashed line). Exo = exothermic.

of crystallized oxide was directly obtained. This finding is confirmed by Shih et al (27), who report that pure ceria precipitate begins to crystallize at 0°C. DSC analysis further confirms this behavior. In fact, the thermograph reported in Figure 1 shows a small and broad exothermic peak at 311°C representing the crystallization of the residual amorphous phase; this peak is also correlated to a very small weight loss. Analyzing the weight loss curve in Figure 1, a low total weight loss (about 8%) can be observed, which can be divided into 2 parts: the first (about 3%) is related to the elimination of adsorbed water, a process that takes place at low temperature, as indicated by the endothermic peak at about 70°C; the second, about 5%, is the weight loss attributable to the thermal dehydration of the hydrous gadolinium-doped ceria. This second step is mainly located between about 200°C and 500°C, albeit a temperature of about 700°C seems necessary for a complete dehydration. This weight loss is quite low compared with a theoretical value of about 17%, calculated in the case of gadolinium-cerium hydroxide with 10% mol of gadolinium, thus indicating that a low degree of hydration is present. This behavior of precipitated ceria is reported also by other authors (25). It is noteworthy that this weight loss is quite low compared with other similar systems, such as yttrium-doped zirconia hydrous gel. Anyway, the very low weight loss in sample C allows us to set up a sintering cycle without any calcination step, as the expected gas evolution during the heating is very low.

To confirm the thermal stability of sample C, in situ XRD analysis at temperatures varying from room temperature to 1200°C was carried out using the Anton Paar HTK 16. The heating rate was 5°C/min, while a dwell time of 10 minutes was set at each temperature before starting the X-ray analysis. These thermal treatments were carried out in air. The relative XRD patterns (not reported here) indicate that no phase transformation took place in sample C during these thermal treatments, and the absence of any peaks belonging to Gd_2O_3, even for firing at 1200°C, confirms the formation of the solid solution between ceria and gadolinia. Obviously

TABLE I - Crystal size of sample C at various temperatures from room temperature to 1200°C

Temperature	Crystal size (nm)
25°C	8.4
200°C	8.3
400°C	10.3
600°C	12.0
800°C	23.7
1000°C	58.1
1200°C	101.1

the grain growth due to the thermal treatment induces an evident sharpening of the XRD peaks, albeit up to 1000°C the peaks are broad enough, thus indicating that the crystallites are still in the nanosize range. Indeed that is confirmed by the crystal sizes calculated by the Scherrer formula for sample C and for the thermally treated samples which are reported in Table I. The crystal size was 8.4 nm at room temperature, and it was nearly constant at 200°C, while it increased up to 101 nm at 1200°C, following a power law model as a function of temperature. Anyway, the solid solution of gadolinium oxide into cerium oxide obtained by coprecipitation is stable over a wide range of temperatures.

The morphology of these powders was analyzed both by SEM (not reported) and TEM. TEM micrograph is shown in Figure 2A. As can be seen, the gadolinium-doped ceria particles were nanosized, about 10 nm, and their size distribution was quite small. The surface area of sample C, measured with the BET method, was 105 m^2/g. From both the surface area and the theoretical density of the materials, it is possible to calculate an average diameter of particles, using the following well-known equation, based on the hypothesis that all of the particles are spherical and with the same diameter:

$$d_p = 6/(\rho\ S)$$

where d_p is the mean particle diameter, ρ is the density (supposed to be equal to 7.22 g/cm^3, the theoretical density of CGO with 10% Gd^{+3} calculated from the crystallographic data reported on ICDD card no. 01-075-0161), and S is the surface area. Using these values, a mean particle diameter slightly lower than 8 nm is found. This value agrees very well with the crystal size of sample C reported in Table I, equal to 8.4 nm. Therefore, from 3 different and independent methods, it was confirmed that sample C was formed by nanosized particles with nanometric crystal size.

Sample C was compacted via cold isostatic pressing at 160 MPa, in cylindrical pellets, and sintered at 1500°C for 3 hours with a heating rate of 10°C/min, while the cooling rate was not controlled. The relative density of this fired sample revealed the very poor densification obtained, with a relative density equal to 74%. The corresponding microstructure, observed by SEM, is not reported here, but it revealed an inhomogeneous material. There were regions of the material that were sintered at a good level, but there were other ones with a very poor densification. The agglomeration phenomena typical of nanometric-size powders very likely induced this behavior. In fact, on heating, the high reactivity of precipitates and coprecipitates promotes a fast coarsening of their primary particles with consequent formation of hard agglomerates (18), and it is well known that the presence of agglomerates leads to heterogeneous packing in the green body, which consequently leads to differential sintering (28).

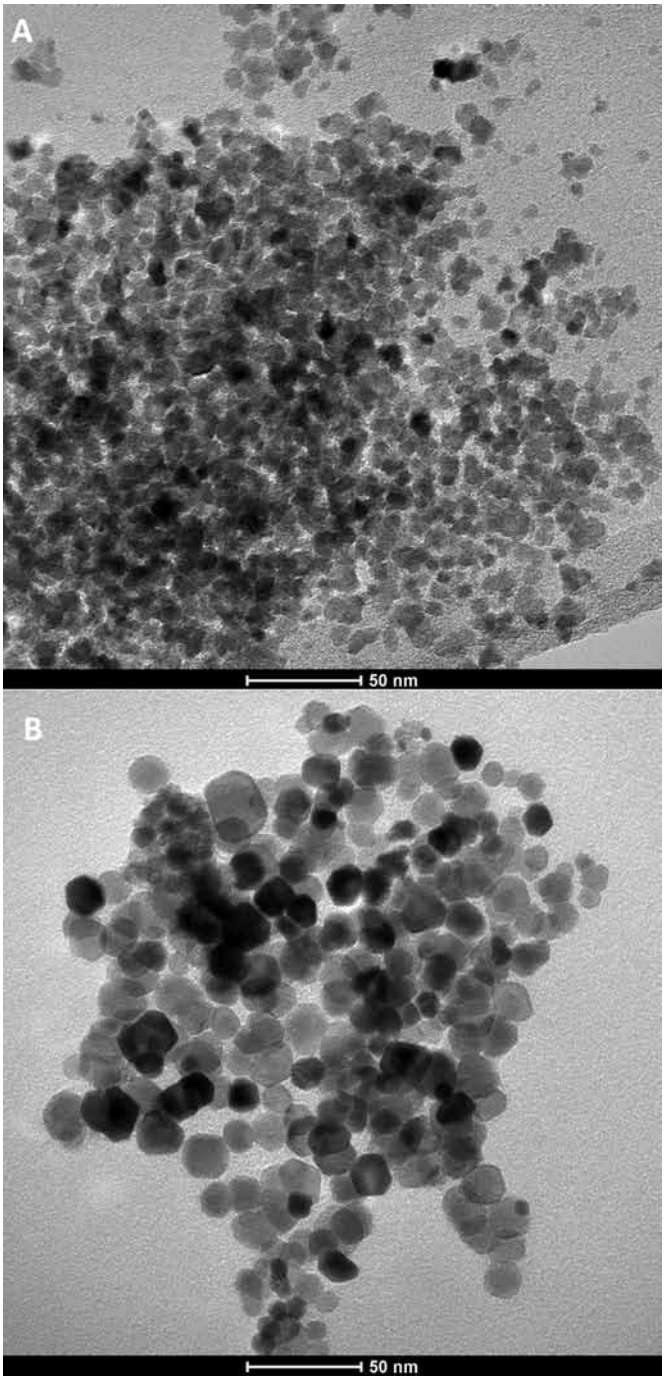

Fig. 2 - Transmission electron microscopy (TEM) micrographs of sample C (**A**) and of sample H_N (**B**).

Thus a typical behavior of other advanced ceramic materials, where the sintering of precipitates and co-precipitates is very difficult to carry out because of the presence of hard agglomerates, was confirmed (15, 16). To improve the sinterability of the coprecipitates, a hydrothermal treatment was carried out using the as-synthesized coprecipitates as precursor, after filtering and washing, but without drying.

Hydrothermal treatments

A first hydrothermal treatment using simply deionized water as mineralizer was carried out at 140°C for 1 day (i.e., sample H_N). The XRD pattern is reported in Figure 3A, and it appears that only the cubic fluorite phase is present. During the hydrothermal treatment, the crystallization process of gadolinium-cerium oxide into the cubic fluorite phase continues, and at the same time, some grain growth phenomena in the nanosized powders occur. The XRD peaks are sharper than those of the precursor, and the crystal size calculated by the Scherrer formula is increased at 16.4 nm. The surface area of sample H_N is nearly half of that found for sample C, with a value of 52.4 m^2/g, which corresponds to a mean particle diameter of about 16.5 nm. The morphology of these powders was observed by TEM, and a micrograph is shown in Figure 2B, where it clearly appears that the particle size is between 15 and 20 nm. Therefore, it is clear that by hydrothermal treatments, individual single-crystal particles of gadolinium-doped ceria are formed, whose size is around 15-20 nm.

To verify the effects of the mineralizer solution on the hydrothermal synthesis of CGO, a second hydrothermal treatment using a solution of 0.1 M of hydrochloric acid (i.e., sample H_A) as mineralizer and a third hydrothermal treatment using a solution of 0.1 M of potassium hydroxide (i.e., sample H_B) as mineralizer, were carried out at 140°C for 1 day. The XRD patterns of samples H_B (Fig. 3B) and H_A (Fig. 3C) confirmed the presence of only cubic ceria. The same present phases and their roughly equal crystallite sizes suggest that for CGO, in contrast to other similar ceramic systems, the hydrothermal crystal growth is almost unaffected by the mineralizer used. However, a different behavior was observed by DTA analysis in samples H_A, H_B and H_N. In fact, as the pH of the mineralizer rose, the samples' total weight loss and temperature of residual amorphous phase crystallization peak rose as well; Table II shows these data, while in Figure 1, the thermograph of sample H_N is given as an example. All 3 thermographs show very small exothermic peaks, representing the residual powder crystallization that is due to the low rate of residual amorphous phase after hydrothermal treatment, albeit different mineralizer affects the temperature of those peaks in an evident manner. In particular, sample H_A has the lowest peak temperature and lowest associated weight loss.

The other effect observed was the different amount of total weight loss of samples H_A, H_N and H_B that can still be divided in 2 parts (elimination of adsorbed water and thermal dehydration of the hydrous gadolinium-doped ceria) as for sample C, but now it is significantly different both in total amount and in proportions between the 2 parts. In fact, for all 3 samples, the second part of weight loss, related to the thermal dehydration of the hydrous gadolinium-doped ceria was always about 5%; but the first, related to adsorbed water, increased from about 2% in sample H_A to about 6% in sample H_B. That is also probably the cause of the increase in residual crystallization peak temperature discussed before.

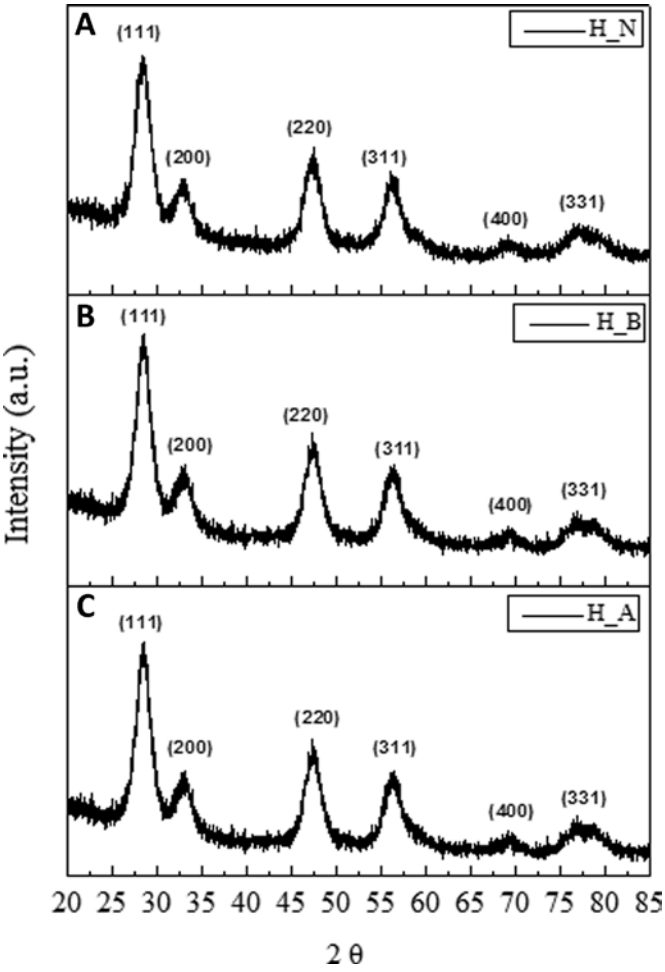

Fig. 3 - X-ray powder diffraction (XRD) patterns for the hydrothermal synthesized samples H_N (**A**), H_B (**B**) and H_A (**C**).

Sintering cycles

To compare the sintering behavior of the as-synthesized CGO (sample C) and of the 3 samples obtained by the hydrothermal treatments, the last ones were compacted in the same way as sample C, and then fired. A first sintering cycle, equal to that used for sintering sample C, was performed on sample H_N. The relative density was 90%, which represented a remarkable improvement with respect to sample C but was still insufficient. Observing the microstructure by SEM, there was again a moderate inhomogeneity in the sample; some regions were very well densified, but in a few other regions, the densification was still poor. However, in this case an optimization of the sintering cycle allowed us to attain a very good densification as the hydrothermally synthesized powders did not suffer the presence of hard agglomerates.

TABLE II - DSC-TGA data for the hydrothermally synthesized samples H_A, H_N and H_B

	H_A	H_N	H_B
Peak temperature (°C)	242.5	297.9	349.0
Weight loss (%)	7.17	8.72	11.07

Indeed, on sample H_A, H_B and again H_N, a different firing cycle was tested as suggested by the thermograph of these samples. To favor the escape of water vapor from the sample during the thermal treatment, heating rates within the range of temperatures in which such an escape occurs, were set at very low values. With a constant temperature of treatment at 1500°C and a duration of 3 hours, the heating was completed in the following way: up to 300°C, the heating rate was set to 3°C/min, between 300°C and 350°C, it was very low, only 1°C/min, to favor the thermal dehydration of sample H_N, and from 350°C to 1500°C, the heating rate was set to 5°C/min.

The results of this "slow" sintering cycle were very interesting. The microstructure of samples H_N was observed by SEM and the relative micrographs are shown in Figure 4, at lower and higher magnifications. The microstructure appears as a relatively uniform, dense and compact ensemble of crystalline grains whose size is in the range 1-2 μm, showing a very good densification of the specimen. A further confirmation of that was given by the relative density which was higher than 0.97 in all 3 samples.

To confirm that the "slow" sintering cycle was able to produce dense products only in the absence of hard agglomerates in the powders, sample C was fired with this sintering cycle. Both the relative density of the compact (about 75%) and the SEM micrograph (not reported here) proved the poor densification of this sample. Moreover, samples H_A, H_N and H_B sintered with the "slow" cycle showed a behavior very similar to each other, with the same microstructure and a comparable relative density. Therefore, the positive effect of hydrothermal treatment in producing nanosized powders without hard agglomerates was confirmed again.

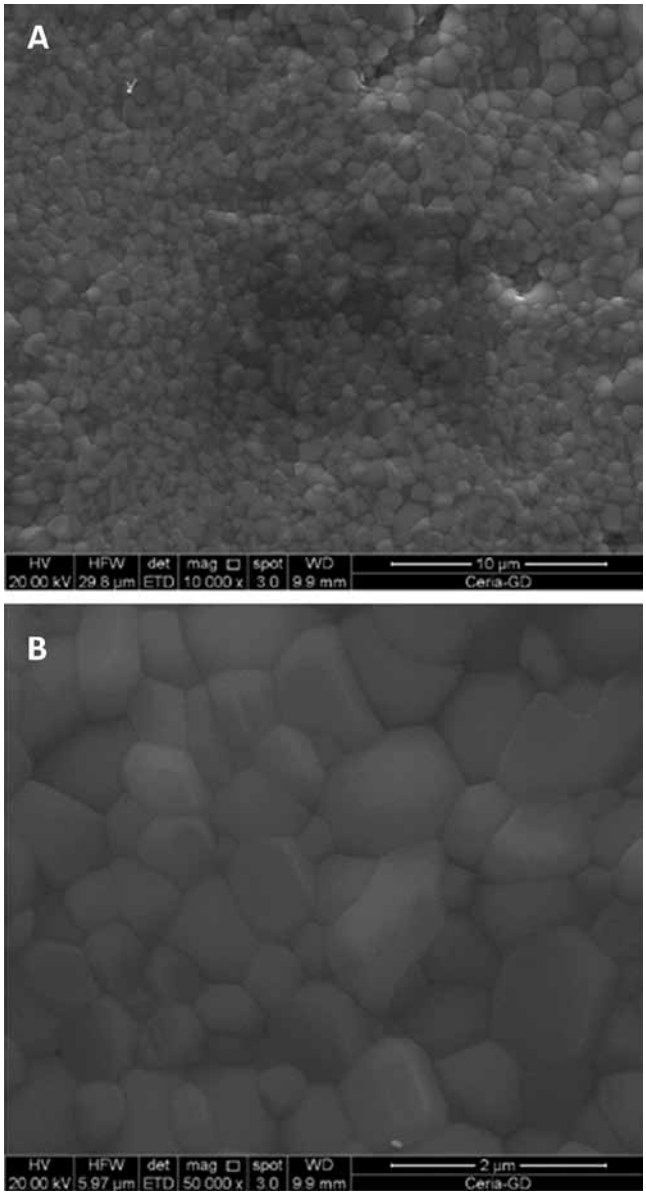

Fig. 4 - Scanning electron microscopy (SEM) micrographs of sample H_N sintered at 1500°C for 3 hours with a slow thermal cycle at lower (**A**) and higher (**B**) magnifications.

Ionic conductivity measurements

The ionic conductivity of the samples H_A, H_N and H_B was determined by AC impedance spectroscopy on a symmetric cell configuration. Electrical properties were achieved using a 2-probe technique. Activation energies (E_a) were calculated by fitting the conductivity data to the Arrhenius relation for thermally activated conduction, which is given as:

$$\sigma = \frac{\sigma_0}{T} \exp\left(\frac{-E_a}{kT}\right)$$

where, E_a is the activation energy for conduction, T the absolute temperature, k the Boltzmann constant and σ_0 the pre-exponential factor.

An impedance plot, referred to as a Nyquist plot, is represented as the negative of the imaginary component of impedance (-Z") versus the real component of impedance (Z'). The plot for a typical polycrystalline material would be generally composed of 3 semicircles, each of which represents a distinct transport process over the range of measurement frequencies (29). The semicircles at higher and lower frequencies represent bulk and electrode responses, respectively, while that at intermediate frequencies represents the grain boundary contribution. Total conductivity will be the sum of different conductivity contributions from bulk, grain boundaries and electrode. This condition of 3 responses is an ideal. The time constants associated with the bulk and grain boundary impedances of most polycrystalline material change with temperature. Therefore, at higher temperatures, for some materials, such as gadolinium-doped ceria, the Nyquist plot shows only the semicircle

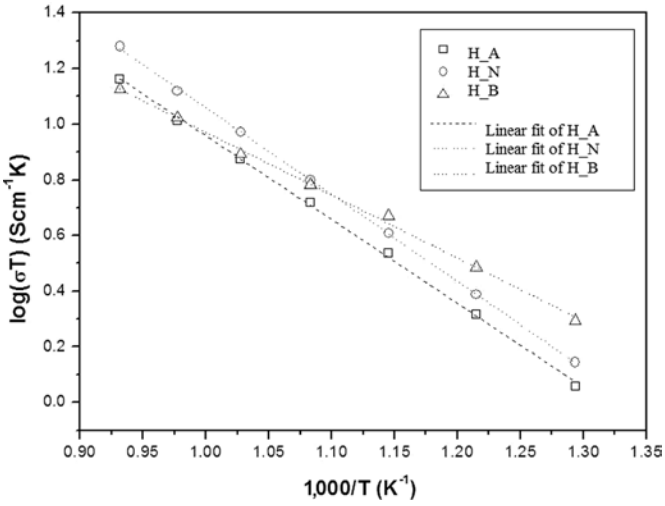

Fig. 5 - Arrhenius plot of samples H_A, H_N and H_B.

due to electrode interfacial processes, because the contribution due to bulk and grain boundary disappears (30).

Therefore impedance spectra measured in the temperature range 500°C-800°C (non reported here) showed a large semicircle due to the electrode process and a tiny semicircle corresponding to grain and grain boundary process at high frequency sides.

To obtain this behavior, the impedance spectra were fitted to a conventional equivalent circuit of 2 parallel combinations of resistance and constant phase elements connected in series. To be compared, resistance was normalized by the electrode area, and was determined by the intercept of the high frequency part of the electrode characteristic on the real axis in the Nyquist plot.

The Arrhenius plots, with linear dependence of log(σT) vs. 1/T, for conductivity of CGO prepared with different hydrothermal treatment, are shown in Figure 5, while the total ionic conductivity derived from impedance spectra for all samples is reported in Table III, for 3 different temperatures.

The fit of the data in the Arrhenius plot is quite good, with a correlation coefficient for a linear squares fit between 0.993 to 0.999. Samples H_A and H_B show very close values above 650°C. In the temperature range 650°C-800°C, the ionic conductivity of H_N was higher than that of the other samples, with a maximum at 800°C of 1.8×10^{-2} S/cm. However, below 650°C, H_B showed the maximum values of conductivity. The decrease in ionic conductivity for H_N could be explained by considering that this temperature was sufficient to define the grain boundary contribution but not low enough to separate the 2 processes. The activation energy was 0.59, 0.61 and 0.57 eV for H_A, H_B and H_N, respectively.

Conclusion

By the coprecipitation method, it was possible to synthesize gadolinium-doped cerium oxide in a fluorite structure, stable in a wide range of temperatures, and which was partially crystallized and partially amorphous and characterized by a very low degree of hydration. This behavior is somewhat different from

TABLE III - Electrical conductivities (S/cm) at various temperatures for the samples H_A, H_N and H_B

Temperature	H_A	H_N	H_B
600°C	0.39×10^{-2}	0.46×10^{-2}	0.61×10^{-2}
700°C	0.77×10^{-2}	0.83×10^{-2}	0.81×10^{-2}
800°C	1.32×10^{-2}	1.80×10^{-2}	1.26×10^{-2}

that of other similar ceramic systems such as zirconia-based precipitates. These ceria powders are nanosized, but their sintering behavior is poor, and a very poor densification is attained. Most likely, this behavior is related to the formation of hard agglomerates, a typical phenomenon in nanosized powders.

Using a hydrothermal treatment directly on the as-synthesized coprecipitates, without any drying step, there was a further crystallization of the fluorite structure with an increasing of the relative crystal size, even if the nanometric character was preserved. Moreover, the hydrothermal treatment had a very positive effect on the powders, which can be sintered with a high degree of densification, as highlighted by the high relative density and by the SEM micrograph of their microstructures.

A sintering cycle with a low heating rate, especially in the range of temperatures where the escape of water vapor is greater, is able to produce very dense ceramic.

The electrical characterization of the samples H_A, H_N and H_B showed that even if their electrical behavior was very similar, some differences appeared in the Arrhenius plots, and in particular, sample H_N was characterized by the highest value of Ea. Thus this sample had the highest electrical conductivity at higher temperatures, and also had the lowest electrical conductivity at lower temperatures – a change of behavior that occurred at about 650°C. It is worth underlining that the electrical conductivities of our samples were very similar to those reported in the recent literature as well (9).

From these results, it appears evident that ceria-based ceramic powders, nanosized, easily moldable, characterized by a very low degree of agglomeration, and therefore able to obtain a very dense ceramic, can be prepared by hydrothermal treatment, and this behavior is almost independent of the mineralizer used. Furthermore, the electrical behavior of these samples is also very interesting, especially with regard to the samples synthesized using neutral mineralizer solution, in the range of higher temperatures, i.e., >650°C, and the samples synthesized using basic mineralizer in the range of low temperatures, i.e., <650°C.

Disclosures

Financial support: No grants or funding have been received for this study.
Conflict of interest: None of the authors has any financial interest related to this study to disclose.

References

1. Hao X, Liy Y, Wang Z, Qiao J, Sun K. A novel sintering method to obtain fully dense gadolinia doped ceria by applying a direct current. J Power Sources. 2012;210:86-91.

2. Munoz F, Gabriela Leyva A, Baker RT, Fuentes RO. Effect of preparation method on the properties of nanostructured gadolinia-doped ceria materials for IT-SOFCs. Int J Hydrogen Energy. 2012;37(19):14854-14863.
3. Sun C, Li H, Chen L. Nanostructured ceria-based materials: synthesis, properties, and applications. Energy Environ. Sci. 2012;5(9):8475-8505.
4. Waldhäusl J, Preis W, Sitte W. Electrochemical characterization of gadolinia-doped ceria using impedance spectroscopy and dc-polarization. Solid State Ion. 2012;225:453-456.
5. Segal D. Chemical synthesis of ceramic materials. J Mater Chem. 1997;7(8):1297-1305.
6. Tessier F, Cheviré F, Muñoz F, et al. Powder preparation and UV absorption properties of selected compositions in the CeO_2–Y_2O_3 system. J Solid State Chem. 2008;181(5):1204-1212.
7. Accardo G, Ferone C, Cioffi R. Influence of lithium on the sintering behavior and electrical properties of $Ce_{0.8}Gd_{0.2}O_{1.9}$ for intermediate-temperature solid oxide fuel cells. Energy Tech. 2016;4(3):409-416.
8. Lee B, Komarneni H, eds. Chemical processing of ceramics. 2nd ed. Boca Raton, USA: Taylor & Francis; 2005.
9. Donmez G, Saritoba V, Altincekic TB, Oksuzomer MA. Polyol synthesis of $Ce_{1-x}RE_xO_{2-x/2}$ (RE = Sm, Gd, Nd, La, 0≤x≤0.25) electrolyte for IT-SOFC. J Am Ceram Soc. 2015;98(2):501-509.
10. Park J, Kim J, Han J, Nam SK, Lim T-H. Hydrothermal synthesis and characterization of nanocrystalline ceria powders. J Ind Eng Chem. 2005;11(6):897-901.
11. Yoshimura M, Byrappa K. Hydrothermal technology past, present and future [review]. J Mater Sci. 2008;43:2085-2103.
12. Dell'Agli G, Colantuono A. Mascolo G. The effect of mineralizers on the crystallization of zirconia gel under hydrothermal conditions. Solid State Ionics 1999;123(1-4):87-94.
13. Dell'Agli G, Mascolo G. Hydrothermal synthesis of ZrO_2-Y_2O_3 solid solutions at low temperature. J Eur Ceram Soc. 2000;20(2):139-145.
14. Dell'Agli G, Mascolo G. Low temperature hydrothermal synthesis of ZrO_2-CaO solid solutions. J Mater Sci. 2000;35(3):661-665.
15. Dell'Agli G, Mascolo G. Agglomeration of 3 mol% Y-TZP powders synthesized by hydrothermal treatment. J Eur Ceram Soc. 2001;21(1):29-35.
16. Dell'Agli G, Mascolo G. Sinterability of 8Y-ZrO_2 powders hydrothermally synthesized at low temperature. Solid State Ion. 2003;160(3-4):363-371.
17. Dell'Agli G, Esposito S, Mascolo G, Mascolo MC, Pagliuca C. Films by slurry coating of nanometric YSZ (8% mol Y_2O_3) powders synthesized by low temperature hydrothermal treatment. J Eur Ceram Soc. 2005;25(12):2017-2021.
18. Dell'Agli G, Mascolo G, Mascolo MC, Pagliuca C. Weakly-agglomerated nanocrystalline $(ZrO_2)_{0.9}(Yb_2O_3)_{0.1}$ powders hydrothermally synthesized at low temperature. Solid State Sci. 2006;8(9):1046-1050.
19. Dell'Agli G, Mascolo G, Mascolo MC, Pagliuca C. Drying effect on thermal behaviour and structural modification of hydrous zirconia gel. J Am Ceram Soc. 2008;91(10):3375-3379.
20. Mascolo MC, Dell'Agli G, Mascolo G. Mesoporous aggregates of ZrO_2-doped (5 mol%) titania by interconnection of primary nano-particles. Microp. Mesop. Mater. 2010;132(1-2):196-200.
21. Tok AIY, Boey FYC, Dong Z, Sun XL. Hydrothermal synthesis of CeO_2 nanoparticles. J. Mat. Proc. Tech. 2007;190(1-3):217-222.
22. Dudek M, Mroz M, Zych L, Drozdz-Ciesla E. Synthesis of ceria-based nanopowders suitable for manufacturing solid oxide electrolytes. Mat Sci Poland. 2008;26(2):319-329.
23. Ivanov VK, Kopitsa GP, Baranchikov AE, Grigorev SV, Runov VV, Haramus VM. Hydrothermal growth of ceria nanoparticles. Russ J Inorg Chem. 2009;54(12):1857-1861.
24. Radovic M, Dohcevic-Mitrovic ZD, Golubovic A, Matovic B, Scepanovic M, Popovic ZV. Hydrothermal synthesis of CeO_2 and $Ce_{0.9}Fe_{0.1}O_2$ nanocrystals. Acta Phys Pol A. 2009;116: 614-617.
25. Dos Santos ML, Lima RC, Riccardi CS, et al. Preparation and characterization of ceria nanospheres by microwave-hydrothermal method. Mater Lett. 2008;62(30):4509-4511.
26. Wang SF, Yeh CT, Wang YR, Wu YC. Characterization of samarium-doped ceria powders prepared by hydrothermal synthesis for use in solid state oxide fuel cells. J Mater Res Technol. 2013;2(2):141-148.
27. Shih CJ, Chen YJ, Hon MH. Synthesis and crystal kinetics of cerium oxide nanocrystallites prepared by co-precipitation process. Mater Chem Phys. 2010;121(1-2):99-102.
28. Rahaman MN. Ceramics processing. Boca Raton, USA: Taylor & Francis; 2007.
29. Accardo G, Ferone C, Cioffi R, Frattini D, Spidigliozzi L, Dell'Agli G. Electrical and microstructural characterization of ceramic gadolinium-doped ceria electrolytes for ITSOFCs by sol-gel route. J Appl Biomater Funct Mater. 2016;14(1):e35-e41.
30. Maricle DL, Swarr TE, Karavolis S. Enhanced ceria: a low temperature SOFC electrolyte. Solid State Ion. 1992;52(1-3):173-182.